International Journal of Automotive Technology, Vol. 5, No. 1, pp. 17–22 (2004)

1229-9138/2004/015-03

EXPERIMENTAL STUDY ON TURBULENT SWIRLING FLOW IN A CYLINDRICAL ANNULI BY USING THE PIV TECHNIQUE

T-H. CHANG*

Division of Mechanical and Automation Engineering, Kyungnam University, Gyeongnam 631-701, Korea

(Received 6 October 2003; Revised 13 January 2004)

ABSTRACT–An experimental investigation was conducted to study the characteristics of turbulent swirling flow in an axisymmetric annuli. The swirl angle measurements were performed using a flow visualization technique using smoke and dye liquid for Re=60,000–80,000. Using the two-dimensional Particle Image Velocimetry method, this study found the time-mean velocity distribution and turbulence intensity in water with swirl for Re=20,000, 30,000, and 40,000 along longitudinal sections. There were neutral points for equal axial velocity at y/(R–r)=0.7–0.75, and the highest axial velocity was recorded near y/(R–r)=0.9. Negative axial velocity was observed near the convex tube along X/(D–d)=3.0–18.0 for Re=20,000.

KEY WORDS : Annuli, PIV, Concave tube, Convex tube, Swirl flow angle

NOMENCLATURE

D : diameter of the concave tube (mm)
d : diameter of the convex tube (mm)
L : xial distance of the swirl chamber (mm)
R : radius of the concave tube (mm)
r : radius of the convex tube (mm)
Re : Reynolds number
S : swirl intensity ($S=1/R[\int_0^r uwr^2dr/\int_0^r u^2rdr]$)
U : time averaged axial velocity (m/s)
u, v, w : fluctuating velocity (m/s)
V : time averaged radial velocity (m/s)
X : axial coordinate of the test tube (mm)
y : radial position from the wall (mm)
θ : swirl angle ($\theta=\tan^{-1}\frac{vw}{uv}$)

1. INTRODUCTION

The flow in a cylindrical annuli, which has been widely utilized in boiler feed water heaters, heat exchangers between sea water and cooling water, tubular type heat exchangers, cyclotron and in cooling the rotor and stator of motors and generators, has been investigated extensively.

The initial investigation, by Rothfus (1948), sought to determine the friction coefficient and velocity profiles of the air flow in the tube, and in the 1949, sought to determine the turbulence intensity, and the Reynolds stress.

In 1964, using a Pitot tube and a hot wire anemometer, Bringhtin *et al.* investigated the mean velocity, turbulence intensity, and Reynolds stress of water in the range of Re=46,000 to 327,000.

Alan Quarmby (1967) measured the friction coefficient and velocity profile of water flow through the test tube for Re=6,000 to 9,000, which had a ratio of R/r= 2.88 to 9.37.

Chigier *et al.* (1964), Scott *et al.* (1973), Milar (1979), Clayton *et al.* (1985) and Reddy *et al.* (1987) studied the swirling flow through a cylindrical annuli by measuring velocity profiles and pressure losses by applying the numerical analysis method. Recently, Chang *et al.* (2001) measured various velocities and Reynolds stress profiles in the horizontal cylindrical tube using the Particle Image Velocimetry method. However, there are seldom investigations with swirl done in this area. Therefore, this study was performed in order to investigate the characteristics of swirl flow through visualization experiments of air flow, which is carried out using smoke and dye in the horizontal annuli of radius ratio R/r=3.0 for Re=60,000–80,000. The time mean velocity and turbulence intensity of the swirling flow in an identical experimental rig were obtained using the two-dimensional Particle Image Velocity method in water as the fluid for Re=20,000–40,000. The present results will contribute to the economical design of heat exchangers.

*Corresponding author. e-mail: changtae@kyungnam.ac.kr

2. EXPERIMENTAL APPARATUS

Figure 1 shows the layout of the experimental apparatus used in this study. Two experimental rigs in same size were employed for this research with air and water. The rigs were manufactured from a acryl tube and a stainless tube. A concave tube diameter of 150 mm and a length of 3,000 mm, a convex tube diameter of 50 mm and a length of 3,000 mm, and a stainless tube with an inner diameter of 50mm and a length of 4,000 mm were used throughout this experiment. The swirl generator was installed at the entrance of the test tube. Because Taurus Controls Ltd. certified their multi-pitot tube for the non-swirling flow but not for the swirling flow, a honey-comb was installed in the front of the multi-pitot tube, and so it was possible for this tube to be use in the swirling flow.

The swirling generator was fabricated using an acryl tube with an outer diameter of 150.0 mm, in which eight holes with a diameter of 3.0 mm were drilled at 45° intervals from the outer to inner tangential direction. In order to adjust the swirling intensity, the swirling generator was designed to be able to move in the swirl chamber. Figure 2 represents a detailed diagram of the cross section of the swirl generator.

For the non-swirling flow experiment, the swirl generator and swirl chamber were dismantled and connected by a guide tube having the same diameter.

Experimental Method and PIV System

In order to determine some of the swirl flow characteristics of the flow induced by the swirl chamber used in this investigation, the flow visualization experiments were carried out first using smoke and dye liquid.

The velocities were measured using the 2-D PIV technique, and the swirl motion of the fluid was produced by a tangential inlet condition. The algorithm used was the gray level cross-correlation method (Kimura *et al.*, 1986). An Ar-ion laser was used and the light from the laser (500 mW) passes through a probe to make a two-dimensional light sheet. In order to make coded images of the tracer particles on one frame, an AOM (Acoustic-Optical Modulator) was used. The AOM controller was synchronized with the camera and a carrier signal was sent to the AOM unit at 100 MHz, which enabled the AOM system to work as an electric shutter, as shown by Kobayashi *et al.* (1991).

The images taken through the camera were captured with a frame grabber (DT3155) and converted into 8 bit levels on the host computer. The particles used in the experiment were nylon 12 (50 mm). For these field images, the velocity vectors were obtained by using the PIV algorithm. The calculation time on the host computer (Pentium 550 MHz) was about 3 minutes in the case of the grid of 35×70, the radius for the searching area was set to 25 pixels, the size for the correlation area was set to

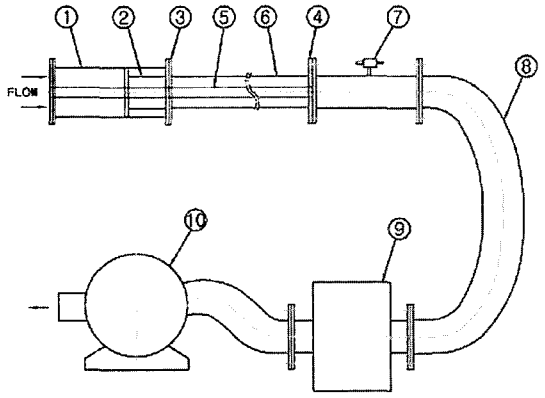

①swirl chamber ②swirl generator ③④teflon flange ⑤convex tube ⑥concave tube ⑦multi-pitot tube ⑧flexible hose ⑨air(or water) chamber ⑩air(or water) pump

Figure 1. Schemetic diagram of the experimental apparatus.

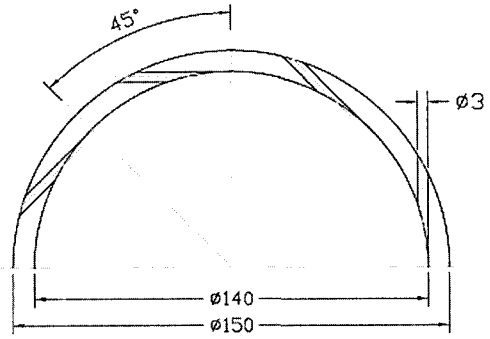

Figure 2. Cross section views through the swirl generator.

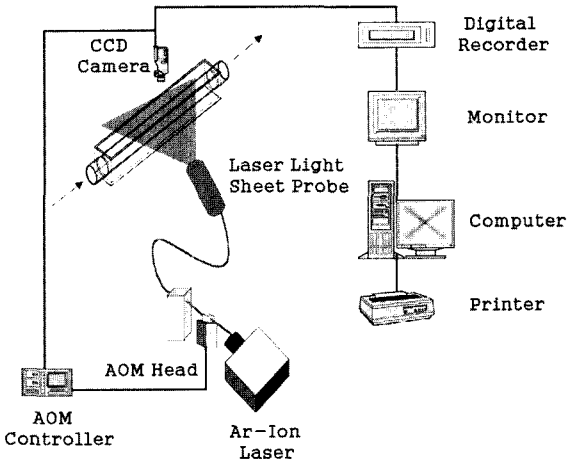

Figure 3. Schemetic arrangement of the PIV system.

32×32 pixels. In order to eliminate erroneous vectors, an error vector elimination method based on the continuous flow condition was adopted.

In order to prohibit the refractive effects of the circular pipe on the results, a square box was installed, which recovered the refracted light waves from the visualized section of the flow. Figure 3 show the diagram of the PIV system used in this experiment.

3. RESULTS AND DISCUSSION

3.1. Swirl Angle Measurement

Several calculations have been performed based on experimental results in order to evaluate the swirl number and define the ratio of angular momentum to linear momentum flux. The 2D PIV technique is used for velocity measurements. Therefore, in the present study, the Reynolds number rather than swirl number is used.

One of the primary objectives of this research was to measure the swirl flow angle along the test tube for different Reynolds numbers. The Reynolds number for these measurements ranged from 60,000 to 100,000 with L/D=0 to 4.

During the flow visualization test, it was observed that some of the water-based liquid used to generate the smoke had condensed. This was deposited on the inside of the concave tube wall in the form of droplets that followed the path of the swirl flow.

Similar results were obtained by Sparrow (1984) who injected an oil lamp black mixture onto white plastic, self-adhering contact paper positioned inside the tube. By removing the paper, the angle made by the flow relative to the tube axis could be measured. In the present experiment, these angles were evaluated by placing a clear plastic sheet over the outside of the concave tube, tracing the streak lines, and then measuring the angle using a method similar to that of Sparrow (1984). The movement of the droplets was, of course, due to the shear stress exerted by the flow at the tube wall. The flow angles were measured at eight pre-selected locations along the length of the test section tube.

The results obtained using smoke for Re=60,000 are shown in Figure 4 In each figure, flow angles are plotted as a function of X/D for both the extreme plenum chamber lengths (L/D=0 and 4). Figure 5 shows the swirl angle using the dye liquid for Re=60,000. Figure 6 illustrates the decay of the swirl angle along the test tube for Re=60,000–100,000 and hence the ratio reduction of the tangential and axial shear stresses. The swirl flow starts with an angle of 70° with respect to the axial direction and decays to 55° at a location close to the end of the test section tube. This angle would have been zero in the case of a pure axial flow. Inspection of the figures shows that θ decreases with X/D, as shown earlier, and that increases in Reynolds number are accompanied by increases in the swirl angle θ.

At any fixed value of X/D and Reynolds number, the swirl angle increases as L/D is increased and as the swirl intensity is increased (i.e. L/D=0 to 4).

From the visualization results, following equation is driven by using the program SPSS (Statistical Package for the Social Science).

$$\theta = 64.285 + (7.216\times10^{-5})\times\mathrm{Re} - 0.633\frac{L}{D} - 0.504\frac{X}{D} \quad (1)$$

This finding was further confirmed a lot of conditions with Reynolds number, X/D and L/D using smoke and dye liquid. The limitation of this equation is available for Re=50,000–120,000 in the horizontal circular annuli.

3.2. Velocity Profiles

Figure 7 shows the time mean velocity vector for Re= 20,000 along the test tube. The velocity vector was indicated as negative values near the convex tube, and then the vectors were showed positive vectors after X/(D-d)=15.0 with decaying swirl intensity. However, a strong

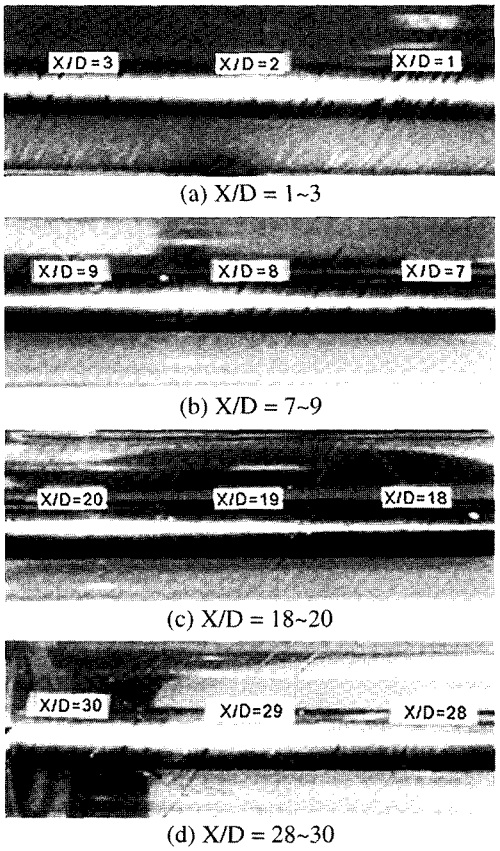

(a) X/D = 1~3

(b) X/D = 7~9

(c) X/D = 18~20

(d) X/D = 28~30

Figure 4. Swirl angle distributions along the test tube using smoke for Re=60,000 at L/D=0.

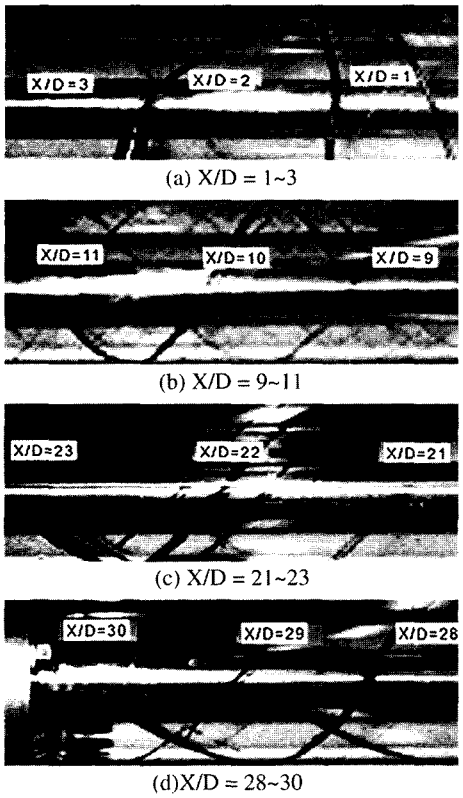

Figure 5. Swirl angle distributions along the test tube using dye liquid for Re=80,000 at L/D=4.

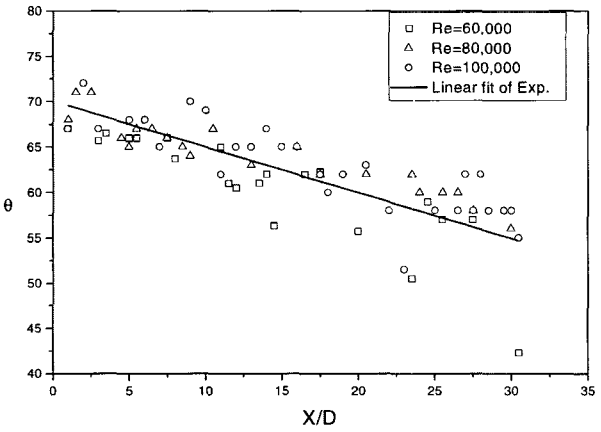

Figure 6. Comparisons of swirl angle for Re=60,000, 80,000 and 100,000 at L/D=0.

vector was observed near the concave tube, and in particular uniform velocity vectors were observed at y/(R-r)=0.7–0.75. The results appeared to be for a similar phenomenon that is not related to Reynolds number. In addition, these gradually disappeared along the test tube.

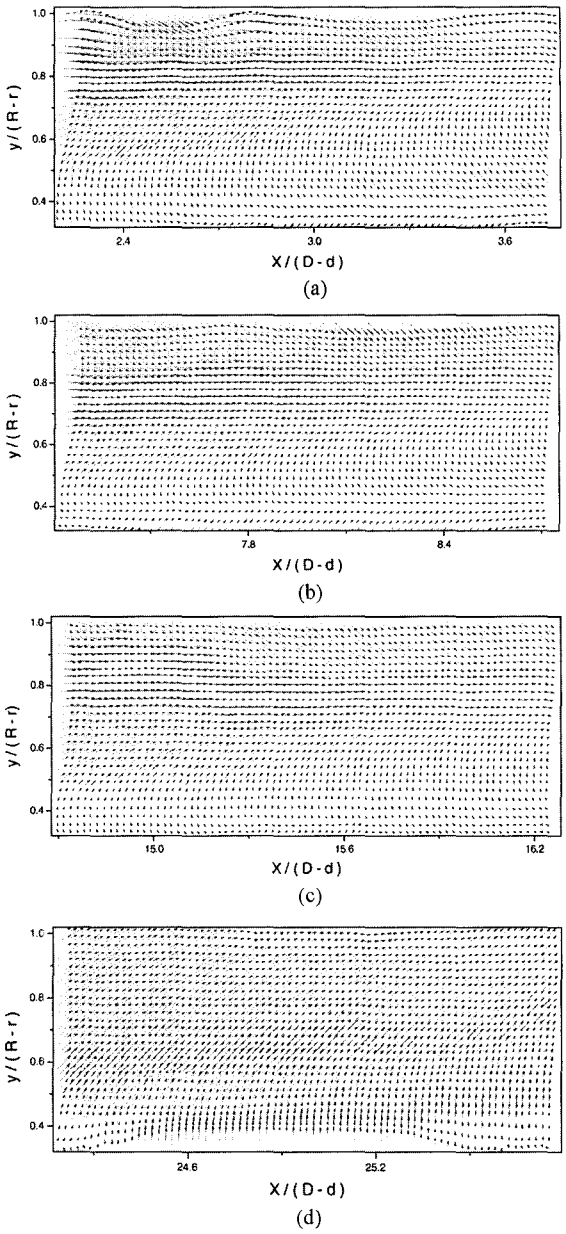

Figure 7. Time-mean velocity vectors with swirl along the test tube for Re=20,000 at (a) X/(D-d)=3.0, (b) 8.0, (c) 15.5, (d) 25.0.

These aspects were related to the decaying tangential velocity with swirl along the annuli. Figure 8 depicts the local axial velocities at X/(D-d)=3, 8, 15.5 and 25 for Re=20,000 that were calculated from the vector shown in Figure 7.

Figure 8 shows the local axial velocity profiles with swirl for Re=20,000 and Re=40,000. The local axial velocities in Figure 8 show negative velocity profiles at X/(D-d)=3.0–18 along the convex tube. The negative

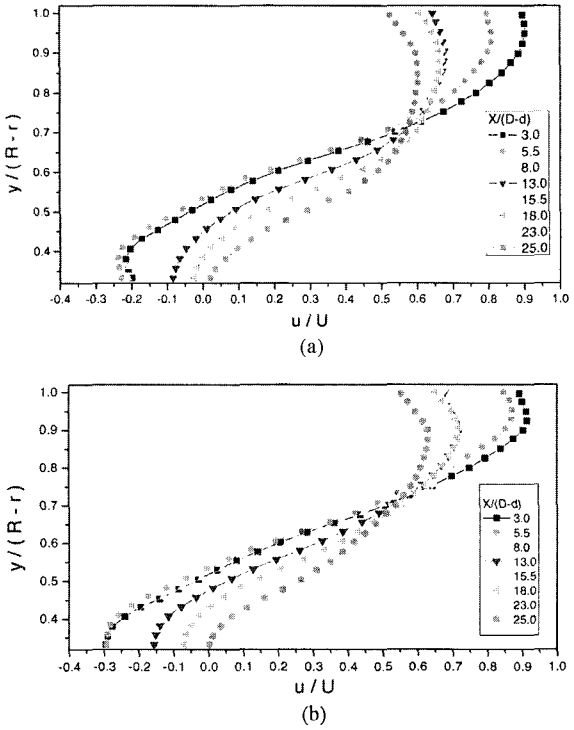

Figure 8. Time-mean axial velocity profiles with swirl along the test tube for (a) Re=20,000 and (b) Re=40,000.

velocity region was increased according to increasing Reynolds number.

However, there is a neutral point for equal velocity at y/(R-r)=0.7–0.75, and the highest velocity near y/(R-r)= 0.9. The maximum velocity point moved to the concave tube by increasing the Reynolds number, but the point also moved to the convex tube by the swirl flow decaying along the test tube. Until now, accurately_measuring the velocity near the wall of a test tube was difficult using hot wire anemometry and LDV.

Unlike in previous research on swirling flow, negative vectors and velocities were observed near the convex tube along X/(D-d)=3–25. Phenomena such as these are similar to those associated with the swirling flow in a horizontal circular tube; however, the velocity gradient is smoother than that of a single tube with a swirl flow. Tangential velocity is thought to have quickly decayed through the concave and convex walls.

3.3. Turbulent Intensity Profiles

Figure 9 depicts the contours of axial turbulence intensity profiles calculated from the vectors for Re=20,000. These intensities show maximum value near the concave wall and at y/(R-r)=0.5. The former indicates the highest axial turbulence intensity near the concave wall as influenced

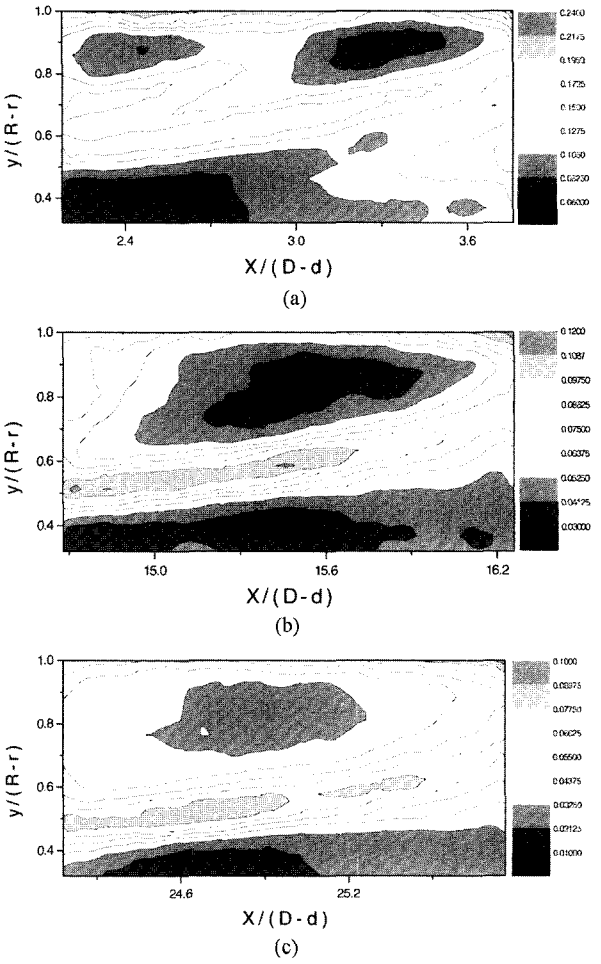

Figure 9. Contours of axial turbulence intensity(u) along the test tube with swirl for Re=20,000 at (a) X/(D-d)=3.0, (b) 15.5 and (c) 25.0.

by tangential velocity and the latter becomes associated with the boundary of the_recirculating zone. These results were observed due to different velocity gradients existing next to each other near the convex wall. However, the axial turbulence intensity was minimal at y/(R-r)=0.8–0.9 and near the convex tube wall. This phenomenon was observed in association with the negative axial velocity.

The contour radial turbulence intensity profiles are plotted in Figure 10. Unlike axial turbulence intensity, these intensities show strong values near the concave and convex tube walls. In addition, these intensities revealed an interesting phenomenon, the lowest radial turbulence intensity was observed near the boundary of the recirculating zone, y/(R-r)=0.5. The results showed a similar phenomenon, although the Reynolds number continued to increase. This is thought to be associated with the strong swirl flow in the horizontal annuli.

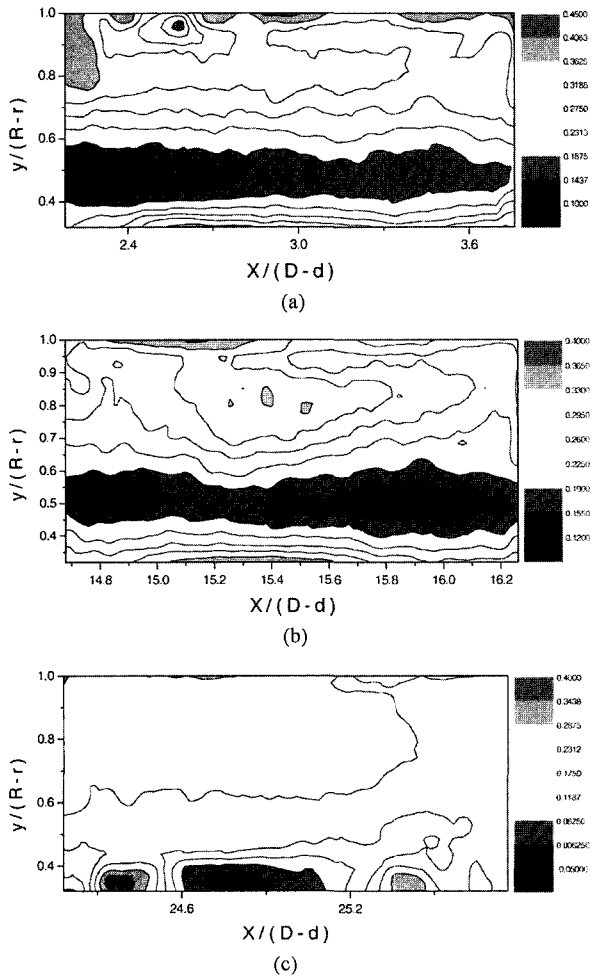

Figure 10. Contours of radial turbulence intensity(v) along the test tube with swirl for Re=20,000 at (a) X/(D-d)=3.0, (b) 15.5 and (c) 25.0.

4. CONCLUSION

Flow visualization using smoke and dye liquid, and velocity measurements by PIV technique were carried out for swirling flow in the horizontal circular annuli. The results obtained in this work are summarized as follows.
(1) The swirl angle was derived from the flow visualization test as equation (1).
(2) The velocity vector had negative values near the convex tube and then the vectors changed to positive velocity after X/(D-d)=15.0 with decaying swirl intensity.
(3) There were neutral points for equal axial velocity at y/(R-r)=0.7–0.75, and the highest axial velocity was recorded near y/(R-r)=0.9. Negative axial velocity was observed near the convex tube along X/(D-d)=3.0–18.
(4) The axial turbulence intensities showed maximum value near the concave wall and at y/(R-r)=0.5.

However, a particular phenomenon was observed when radial turbulence intensities were being investigated. The lowest intensity was noted near the boundary of the recirculating zone, y/(R-r)=0.5.

ACKNOWLEDGEMENT–This work was supported by a Kyungnam University research fund, 2003.

REFERENCES

Alan Quarmby. (1967). An Experimental study of turbulent flow through concentric annuli. *Int. J. Mech. Sci.*, **9**, 205–221.

Brighton, J. A. and Jones, J. B. (1964). Fully developed turbulent flow in annuli. *J. of Basic Eng.* **86**, 835–844.

Chang, T.-H. and Kim, H.-Y. (2001). An investigation of swirling flow in a cylindrical tube. *KSME Int. J.* **15**, **12**, 1892–1899.

Chighier, A. N. and Beer, J. M. (1964). Velocity and static - pressure distributions in swirling air jets issuing from annular and divergent nozzle. *ASME, J. of Basic Engineering*, 788–796.

Clayton, B. R. and Morsi, S. M. (1985). Determination of principal characteristics of turbulent swirling flow along annuli. *Int. J. Heat & Fluid Flow* **6**, **1**, 31–41.

Kimura, I. and Takamori, T. (1987). *Image Processing of Flow Around a Circular Cylinder by using Correlation Technique*. Flow Visualization IV. Hemisphere Pub. Tokyo, Japan. 22–226.

Kobayashi, T., Saga, T., Haeno, T. and Tsuda, N. (1991). Development of a real-time velocity measurement system for high Reynolds fluid flow using a digital image processing design, experimental and numerical flow visualization (Ed Khalighia B. *et al.*). *ASME FED*, **128**, 9–14.

Milar, D. A. (1979). A Calculation of laminar and turbulent swirling flows in a cylindrical annuli. *ASME*, Winter Annual Meeting, New York, Dec. 89–98.

Reddy, P. M., Kind, R. J. and Sjolander, S. A. (1987). Computation of turbulent swirling flow in an annular duct., *Numumerical Method in Laminar and Turbulent Flow*, 470-481.

Rothfus, R. R. (1948). Velocity distribution and fluid friction in concentric annuli. Ph.D Thesis, *Carnegie Institute of Technology*, U.S.A.

Scott, C. J. and Raske, D. R. (1973). Turbulent viscosities for swirling low in a stationary annulus. *ASME, J. of Fluid Engineering*, **95**, 557–566.

Sparrow, E. M. and Chaboki, A. (1984). Swirl-affected turbulent fluid flow and heat in a circular tube. *J. of Heat Transfer, ASME*, **106**, 766–773.